Desalination and Water Treatment
www.deswater.com

doi: 10.5004/dwt.2017.20403

67 (2017) 105–111
March

Change of crystal size and interplanar spacing of $CaCO_3$ in adherent and non-adherent scale by forced-convection heat transfer

Zhi-An Liu[a], Tian Xia[a], Ju-Dong Zhao[b,*], Wen-Bo Ma[a], De-Hao Kong[a], Xing Yang[a], Xiao-Jue Shao[a]

[a]*College of Energy and Power Engineering, Inner Mongolia University of Technology, Hohhot 010051, China, Tel. +86-471-6576145; email: lza1232003@aliyun.com (Z.-A. Liu), Tel. +86 13944672349; email: 475239599@qq.com (T. Xia), Tel. +86 15802412476; email: 396058779@qq.com (W.-B. Ma), Tel. +86 15848195963; email: 564335884@qq.com (D.-H. Kong), Tel. +86 15248078051; email: 270788680@qq.com (X. Yang), Tel. +86 18847168335; email: 349869317@qq.com (X.-J. Shao)*
[b]*College of Science, Inner Mongolia University of Technology, Hohhot 010051, China, Tel. +86-471-6576370; email: jdzhao@imut.edu.cn*

Received 16 May 2016; Accepted 30 November 2016

ABSTRACT

A simple device to simulate circulating cooling water was used to study the dynamic reactions of two scale types. Water velocity, which ranged from 0.401 to 1.338 m/s, was adopted to study the effects on crystal size and interplanar spacing of adherent and non-adherent scale. The adherent scale was deposited on copper pipe surface. By using X-ray diffraction, the results suggest that the crystal size of calcite and aragonite in adherent scale increased by ca. 200–300 Å and 100–200 Å, respectively, when compared with that of corresponding non-adherent scale. As water velocity increased, the crystal size of adherent scale increased, while the crystal size of non-adherent scale remained essentially unchanged. Analysis of the change of crystal size and mass fraction showed that stronger hydraulic force was needed to remove calcite, as compared with the removal of aragonite. The data also confirmed that the interplanar spacing of adherent scale was smaller than that of non-adherent scale, as a result of saturation and temperature.

Keywords: Circulating cooling water; Adherent scale; Non-adherent scale; Crystal size; Interplanar spacing; X-ray diffraction

1. Introduction

Buildup of scale encrusting the surface of heat exchangers is initiated by heating and decomposition of $Ca(HCO_3)_2$ in water. As a result, calcium carbonate ($CaCO_3$) precipitates and eventually forms calcite and aragonite scale. Based on physics and chemistry, scale buildup can be divided into six categories: crystallization, particle formation, chemical reaction, corrosion, microbiological, and solidification fouling. The most common type of scale buildup in heat-exchange systems is crystallization fouling formed from the crystallization of $CaCO_3$ [1]. This is a complex physical and chemical process involving energy, mass, and momentum transfer.

Some recent reports have discussed the characteristics and effects of $CaCO_3$ scale. Dalas and Koutsoukos [2] investigated the crystallization process of $CaCO_3$ solution under a magnetic field exceeding 10 T, and revealed that a strong retardation is observed on the crystallization of calcite, and the rates of crystallization decreases with increase of field intensity. Both theoretical and experimental investigations indicated that the calcite/aragonite/vaterite ratio varies by changing the strength of the field and the flow rate of the water through the system [3]. The effect of permanent magnetic field on $CaCO_3$ precipitation type and solubility were investigated and found that magnetic treatment increases

* Corresponding author.

1944-3994/1944-3986 © 2017 Desalination Publications. All rights reserved.

the total amount of precipitate and favors the homogeneous nucleation depending on water treatment: pH, water flow rate, and the residence time [4]. Recently, the effectiveness of electromagnetic fields was investigated in preventing $CaCO_3$ fouling in cooling water, and found that particle size became small and the crystal structure changed into loose style after the electromagnetic anti-fouling treatment [5]. When $CaCO_3$ crystals were treated in a 4.0 kV high-voltage electrostatic field, An et al. [6] discovered that the formation of aragonite is induced. Moreover, the combined effect of high voltage electrostatic and variable frequency pulsed electromagnetic fields on $CaCO_3$ precipitation was studied both by experimentally and theoretically, and suggested that this effect favors the appearance and growth of aragonite, and restrains its transition to calcite [7]. Lee [8] investigated water treated with an alternating electromagnetic field and revealed that the electromagnetic field contributes to larger crystal size and aragonite transformed from calcite is easily washed away. The effects of permanent magnetic field on $CaCO_3$ scaling of circulating water were reported and it was found that the existence of magnetic field increases the nucleation rate of $CaCO_3$, and inhibits crystal particle growth [9]. Moreover, the effects on pipe material for $CaCO_3$ precipitation were assessed by means of a precipitation test, and the pipe materials strongly influences the nucleation process of $CaCO_3$ [10]. For $CaCO_3$ scale, the inhibition effects of maleic anhydride copolymers as scale inhibitors in copper pipe were better than that in stainless steel [11]. Effects of different operating parameters on crystallization fouling of $CaCO_3$ on a flat heat transfer surface were studied to find out their effects on controlling fouling mechanism [12]. Then, the researchers have modeled $CaCO_3$ crystallization fouling on a heat exchanger surface, and found that the effect of fluid velocity should be included in the model [13].

These reports confirm that (1) the formation of encrustation scale in solution is controlled by crystallization kinetics of nucleation and growth in relation to the degree of supersaturation, ion type, temperature, pH, and physical and chemical properties of crystal surface; (2) the supersaturation or partial supersaturation of $CaCO_3$ in solution is the precondition for precipitation and crystallization of $CaCO_3$; and (3) vaterite and aragonite are usually the first phase of precipitation and crystallization.

During dynamic heat transfer, some $CaCO_3$ crystals deposit on the surface of containers as adherent scale, while the rest are flushed away by water as non-adherent scale. However, few studies have reported on the morphology of adherent and non-adherent crystal scale, including crystal size and interplanar spacing. Moreover, recent studies have focused on the nucleation process of $CaCO_3$, but ignored the dynamics of adherent and non-adherent scale formation. Therefore, in the present paper, an experimental device was developed to analyze the crystal morphologies of adherent and non-adherent scale by XRD.

2. Experimental setup

The experimental device and its working principles are shown in Fig. 1. Forced-convection heat transfer was adopted in this experiment. The nominal inner diameter of heat-exchange copper tubing is 25 mm, the nominal out diameter is 27 mm, and the effective heat-exchange length is 565 mm. The volume of circulating cooling water is 0.161 m^3. The diameter and height of the cooling tower are 400 and 1,500 mm, respectively. A packing layer of polyhedral and hollow polypropylene spheres of Φ50 mm was placed in the tower. The axial flow ventilator operated at a rate of 4,000 m^3/h. A sieve with pore diameter ≤38 μm was used to intercept non-adherent scale. The adherent scale sample was taken from the surface of heat-exchange copper tubes, while the non-adherent scale sample was taken from the sieve.

The temperature of circulating cooling water was kept at 30°C ± 0.5°C, and the heating temperature was set at 90°C ± 0.5°C. Water quality is given in Table 1. The whole process was performed within 28 h. During the formation of scale in this experiment, the concentration of Ca^{2+} and HCO_3^- was decreased. In order to maintain a stable hardness and alkalinity of circulating cooling water, AR grade (99.9+ %) $CaCl_2$ with a constant flow rate of 2.1 mmol / (L·h) and AR grade $NaHCO_3$ with a constant flow rate of 2.3 mmol / (L·h) were used to compensate for the loss of Ca^{2+} and HCO_3^-,

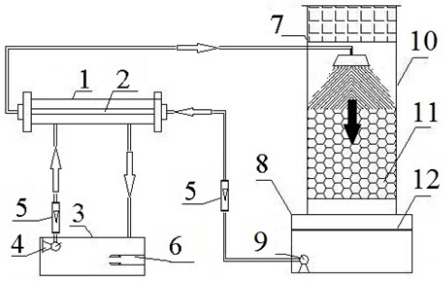

1-Force convection heat exchanger
2-Heat-exchange copper tubing
3-Calorifier
4-Heater lift pump
5-Electromagnetic flow meter
6-Electrical bar
7-Axial flow ventilator
8-Tower pond
9-Circulating water pump
10-Cooling tower
11-Packing layer
12-Sieve

Fig. 1. The experimental device, working principles, and process of scale formation.

respectively. $CaCl_2$ and $NaHCO_3$ were produced by Tianjin Fengchuan Chemical Reagent Technologies Co., Ltd.

Four water velocities, including 0.401, 0.669, 0.870, and 1.338 m/s, were implemented to observe the flow-dependent change of crystal morphology. Two parallel experiments were conducted for each water velocity.

Table 1
Water quality

Water quality	Value
Ca^{2+}, mmol/L	6.21
Total hardness (*H*), mmol/L	7.58
Alkalinity (*A*), mmol/L	6.03
Cl^-, mmol/L	8.91
Mg^{2+}, mmol/L	1.37
Conductivity, μS/m	1,217
pH	7.23

3. Results and discussion

After the experiment, both adherent and non-adherent scale types were collected, respectively. The samples were put in a 105°C oven for 24 h to eliminate water and then ground in a mortar and sieved by a 200 mesh nylon sieve. Analysis was performed by X-ray diffractometer (D/MAX-2500/PC, Rigaku, Japan).

3.1. XRD results

Phase indentifying of experimental scale is shown in Fig. 2.

Generally, the peaks corresponding to (104), (018), and (116) crystal planes had relatively strong intensities, while intensity of the (104) plane was the strongest. Therefore, the (104) plane could be used to collect information about calcite. In the XRD spectrum of aragonite, (111), (021), and (221) crystal planes had strong peak intensities. Since the (111) peak was the strongest, it was used to analyze aragonite crystals.

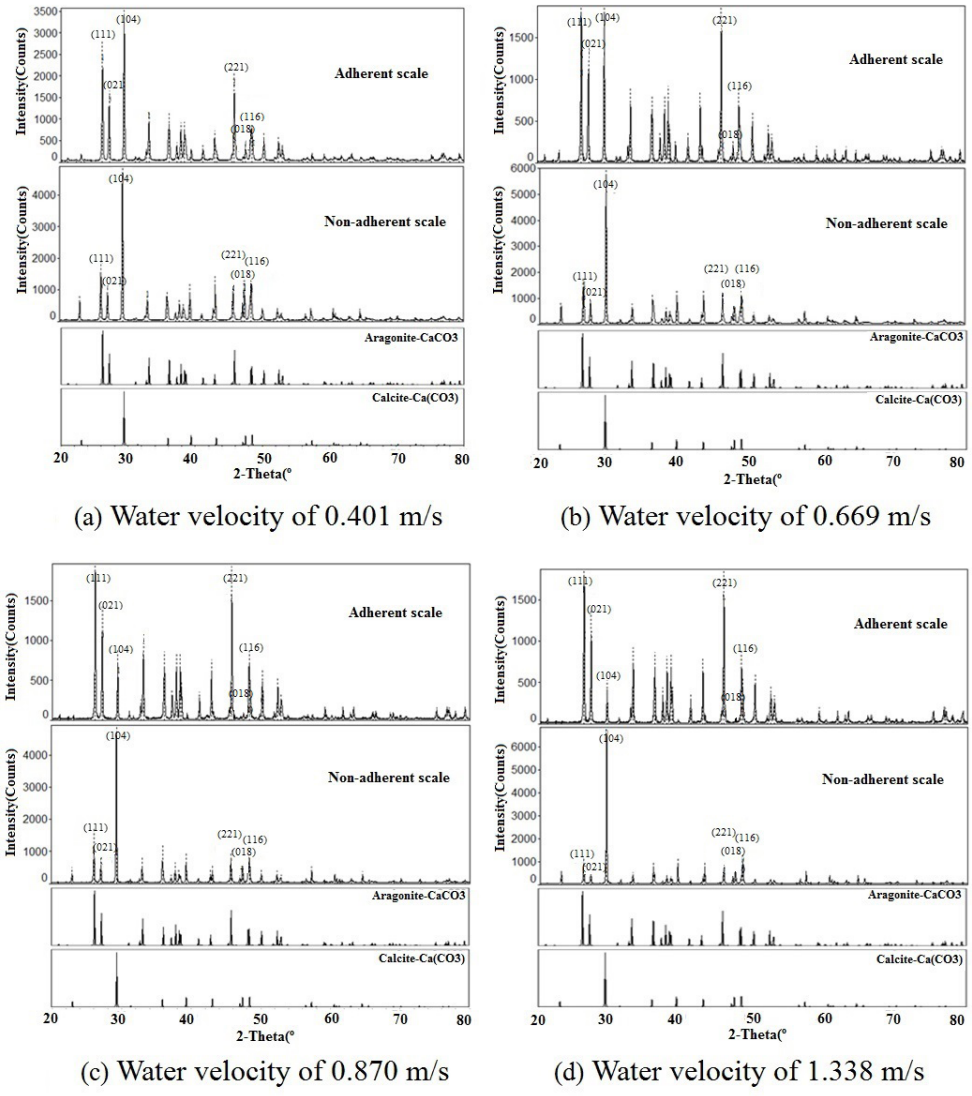

Fig. 2. Phase identifying spectrum of experimental scale vs. different water velocity.

Two parallel experiments were performed for each water velocity, XRD results of eight experiments are given in Table 2 and show that aragonite and calcite are the main phases in encrustation scale. The strongest characteristic peaks of (111) and (104) appeared at 26.2° and 29.4°, corresponding to aragonite and calcite, respectively. Compared with adherent scale, the characteristic peaks of non-adherent scale shifted to lower angle side. The average offsets for aragonite and calcite were 0.015° and 0.035°, respectively, which may have been caused by the increased interplanar spacing of non-adherent scale. This was also suggested by the previous experiment [9].

3.2. Change of crystal sizes

From XRD analysis, it could be clearly seen that the crystal sizes of scale had changed. D_{hkl} stands for the crystal size perpendicular to crystal plane (*hkl*). The curves of D_{104} of calcite and D_{111} of aragonite vs. water velocity are given in Figs. 3 and 4, respectively.

3.2.1. Differences of crystal size in adherent and non-adherent scale

In the process of circulation, the micrograins, which were flushed away by water, were observed in the sieve, forming the non-adherent scale. Because the sieve was immersed in the tower pond, in which the water temperature was kept in 30°C ± 0.5°C, crystal growth is slow, leading to a small crystal size of non-adherent scale. At high temperature (90°C ± 0.5°C) of heat-exchanger wall, the solubility of $CaCO_3$ is reduced and the water solution can be easily supersaturated, satisfying the necessary condition of crystallization. This maintains the stable crystal growth of adherent scales deposited on the surface of copper tubes in the heat exchanger. Hence, the crystal size of adherent scale was generally larger than that of non-adherent scale.

During the recrystallization of $CaCO_3$ solution, crystals gradually grew. After recrystallization, crystal growth normally develops under continual heating or thermal preservation. With interface curvature as the driving force, the

Table 2
XRD results

v (m/s)	Scale sample	Phase	*hkl*	2θ	*d* (Å)	*I* (%)	*D* (Å)
0.401	Adherent	Aragonite	111	26.199	3.3986	100.0	592
		Calcite	104	29.402	3.0353	91.0	720
	Non-adherent	Aragonite	111	26.182	3.4009	24.9	584
		Calcite	104	29.382	3.0373	100.0	764
0.401	Adherent	Aragonite	111	26.199	3.3986	64.2	595
		Calcite	104	29.419	3.0335	100.0	663
	Non-adherent	Aragonite	111	26.161	3.4034	32.2	562
		Calcite	104	29.363	3.0392	100.0	753
0.669	Adherent	Aragonite	111	26.181	3.4010	100.0	656
		Calcite	104	29.400	3.0355	54.8	818
	Non-adherent	Aragonite	111	26.161	3.4036	24.3	590
		Calcite	104	29.364	3.0391	100.0	759
0.669	Adherent	Aragonite	111	26.201	3.3984	9.2	663
		Calcite	104	29.419	3.0336	100.0	787
	Non-adherent	Aragonite	111	26.163	3.4033	28.9	595
		Calcite	104	29.362	3.0393	100.0	733
0.870	Adherent	Aragonite	111	26.184	3.4005	100.0	689
		Calcite	104	29.403	3.0352	36.8	909
	Non-adherent	Aragonite	111	26.159	3.4037	23.8	619
		Calcite	104	29.378	3.0377	100.0	677
0.870	Adherent	Aragonite	111	26.199	3.3987	97.9	724
		Calcite	104	29.418	3.0336	100.0	1,000
	Non-adherent	Aragonite	111	26.161	3.4035	17.6	581
		Calcite	104	29.380	3.0375	100.0	805
1.338	Adherent	Aragonite	111	26.177	3.4015	100.0	762
		Calcite	104	29.414	3.0341	23.1	1,000
	Non-adherent	Aragonite	111	26.143	3.4059	13.1	599
		Calcite	104	29.361	3.0395	100.0	720
1.338	Adherent	Aragonite	111	26.159	3.4037	100.0	843
		Calcite	104	29.378	3.0377	52.2	1,000
	Non-adherent	Aragonite	111	26.180	3.4011	8.9	636
		Calcite	104	29.362	3.0393	100.0	725

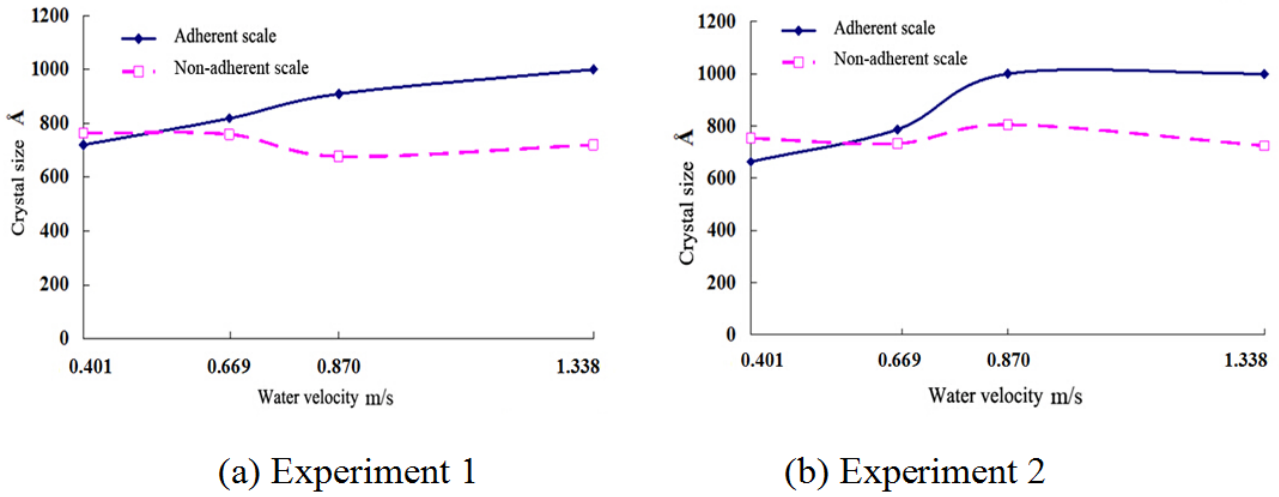

Fig. 3. Curves of D_{104} of calcite vs. water velocity.

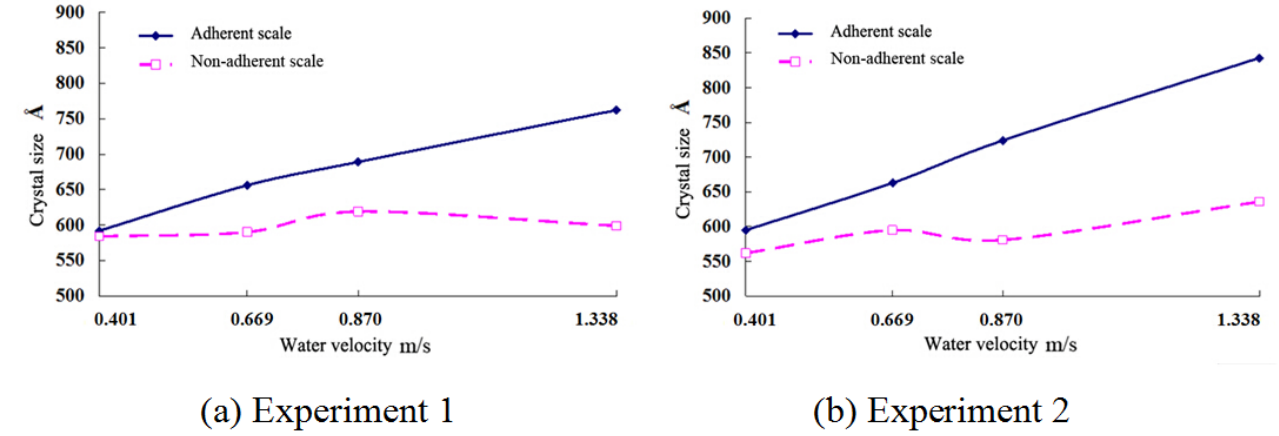

Fig. 4. Curves of D_{111} of aragonite vs. water velocity.

balanced growth of crystals is promoted. Within a certain temperature range, crystal size is roughly the same with little fluctuation. However, as temperature rises, mean crystal size increases, and crystal growth can be considered as an interface migration process whereby the interface curvature propels the movement of bending interface toward the center of curvature to minimize energy. Therefore, it can be concluded that temperature affects the migration rate of crystal interface and that higher temperature causes greater migration rate of crystal interface, resulting in faster crystal growth rates. This is in good agreement with previous results [14].

$CaCO_3$ with smaller crystal size was easily washed away by water to form non-adherent scale, for both calcite and aragonite, while $CaCO_3$ with larger crystal size tended to deposit on the surface of heat transfer to form adherent scale, also for both calcite and aragonite. Liu [15] has also found that microcrystals tended to form under an alternating electromagnetic field and were more apt to be washed away rather than deposited on the surface, thus showing anti-scale effect.

3.2.2. Effect of water velocity on crystal size of adherent and non-adherent scale

From Table 2, it can be observed that the crystal size of adherent and non-adherent scale increased with increasing water velocity. The crystal size of calcite increased from 663 to ≥1,000 Å, while the crystal size of aragonite increased from 592 to 843 Å. However, the change of crystal size of non-adherent scale was not as remarkable. The crystal size of calcite was between 677 and 805 Å, while that of aragonite in non-adherent scale was between 562 and 636 Å showing a flat trend.

The above phenomena indicates that the smaller crystals of $CaCO_3$ were easily flushed by water, resulting in the larger crystal size of adherent scale under increased water velocity and enhanced washing effect. On the other hand, non-adherent scale on the sieve grew slowly as a result of the constant temperature, which produced a relatively uniform crystal size. Based on the relationship between water velocity and crystal size of adherent and non-adherent scale, it can be inferred that only $CaCO_3$ crystal within an appropriate size range can form non-adherent scale. Otherwise, it will form adherent scale.

3.2.3. Stronger hydraulic conditions are needed to avoid calcite-type scale

For calcite-type scale, the crystal size of adherent scale was smaller than that of non-adherent scale when low water velocity of 0.401 m/s was used. When higher water velocities of 0.669, 0.870, and 1.338 m/s were adopted, the crystal size of adherent scale was larger than that of non-adherent scale by roughly 200 and 300 Å. For aragonite scale, adherent and non-adherent scale shared about the same crystal size range when a lower water velocity of 0.401 m/s was used. Higher water velocities between 0.669 and 1.338 m/s led to increased crystal size of adherent scale by about 100–200 Å, compared with non-adherent scale.

Several factors contribute to these changes. When water velocity was 0.401 m/s, water flushing had a weaker effect on the removal of calcite, allowing calcite with smaller crystal size to deposit more easily on the surface of the heat exchanger to form adherent scale. Under these conditions, the crystal size of adherent scale was smaller than that of non-adherent scale. When water velocity was equal to or greater than 0.669 m/s, water flushing began to influence the deposition of calcite-type adherent scale, and the crystal size of adherent scale was larger than that of non-adherent scale. When all the considered water velocities were applied, water flushing had a remarkable effect on the prevention of aragonite-type scale. So, the crystal size of adherent scale was larger than that of non-adherent scale. It can be concluded that water flushing can be used to remove both calcite and aragonite scale. From Table 2, it is clearly to see that the crystal size of calcite is larger than that of aragonite at the same water velocity. Therefore, to remove calcite, higher water velocity and larger shearing stress are required. This agrees with that the shear forces at the wall may prevent the crystals to attach to the surface when the flow velocity is high [12].

Ferreux [16] found that a magnetic field could change the enthalpy of formation for $CaCO_3$. The aragonite initially formed under a magnetic field had a needle-like shape and was difficult to deposit on the bottom of containers, allowing it to be washed away more easily by fluids. This further confirms the above-mentioned phenomenon.

3.3. The change of interplanar spacing

The differences between adherent and non-adherent scale are manifested by crystal size and interplanar spacing. The d_{104} stands for interplanar spacing of the (104) plane in calcite, and d_{111} is the interplanar spacing of the (111) plane in aragonite. The curves of d_{104} of calcite and d_{111} of aragonite vs. water velocity are given in Figs. 5 and 6, respectively. As shown in these two figures, the interplanar spacing of both calcite and aragonite in non-adherent scale was larger than that of adherent scale. This may be explained by the theory of crystal growth [17], which proposes that supersaturation is necessary for recrystallization in solution. The saturability of $CaCO_3$ crystal at the point of recrystallization is defined as the critical supersaturation degree, which must be surpassed before the recrystallization of $CaCO_3$. Degree of saturability (SR) is commonly used to denote the saturability of a solution. For $CaCO_3$ solution, the SR can be calculated by Eq. (1):

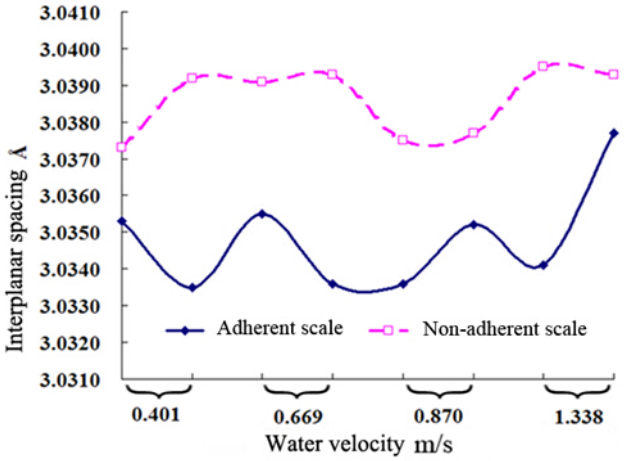

Fig. 5. Curves of d_{104} of calcite vs. water velocity.

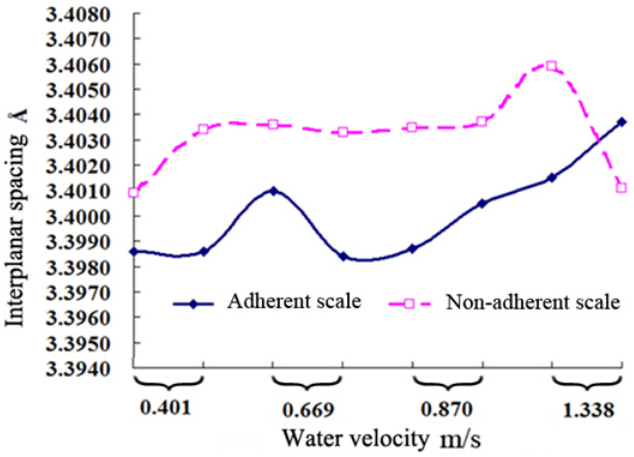

Fig. 6. Curves of d_{111} of aragonite vs. water velocity.

$$SR = \left(\alpha\left(Ca^{2+}\right)\cdot\alpha\left(CO_3^{2-}\right)\right)/K_{sp} \quad (1)$$

where α is activity, mol/L, and K_{sp} is solubility product, mol^2/L^2.

It is assumed that the saturation point of $CaCO_3$ solution has been reached when the SR is equal to 1. It is possible for $CaCO_3$ crystals to crystallize when the SR is greater than 1, but this recrystallization process does not proceed instantaneously. Recrystallization will only be promoted at a SR larger than a certain value.

Previous studies have analyzed the change of precipitation rate of calcite and aragonite, giving a relative order of precipitation that depends on various values of temperature and pressure [18–21]. According to the theory of homogeneous crystal formation, crystallization rate J can be expressed by Eq. (2):

$$J = A\exp\left[-\frac{\beta N_A \sigma^3 V_m^2}{R^3 T^3 (\ln SR)^2}\right] \quad (2)$$

where A is constant, β is lattice constants, σ is surface free energy, V_m is molecular volume, N_A is Avogadro's number, R is the gas constant, T is temperature, and SR is the degree of saturability.

At the surface of the heat exchanger, high temperatures cause high SR for $CaCO_3$ solution. Based on Nielsen's theory [22], crystallization rate is greatly enhanced when the SR reaches a certain value, as noted above. Therefore, the crystallization rate of adherent scale on the surface of a heat exchanger is much higher than that on the sieve surface. As growth continues, some particles which were out of order begin to participate in the ordered arrangement in adherent scale. As a result, more ordered structures in the crystal, stronger attractive force between particles in the lattice, and smaller interplanar spacing all occur.

During the initial growth period, non-adherent scale is carried away to the sieve by water flushing. At this point the relatively low temperature promotes a low SR of $CaCO_3$ and a low crystallization rate. This decreases the amount of particles in the ordered crystal structure and the attraction force between particles, which leads to the increase of interplanar spacing. Therefore, it can be inferred that the interplanar spacing in adherent scale is smaller than that in non-adherent scale.

4. Conclusions

$CaCO_3$ with smaller crystal size is easily washed away by water to form non-adherent scale, while $CaCO_3$ with larger crystal size tends to deposit on the surface of the heat exchanger to form adherent scale. Water flushing can remove calcite- and aragonite-type scale as non-adherent scale, and higher water velocity induced stronger hydraulic flushing, is necessary to remove calcite. Different values of SR, T, and σ of adherent and non-adherent scale cause the crystallization rate of adherent scale to be higher than that of non-adherent scale, which, in turn, decreases interplanar spacing in adherent scale.

Acknowledgments

This project was supported by National Natural Science Foundation of China (51068020, 51268040) and Inner Mongolia Graduate Student Scientific Research Innovation Projects (S20141012815).

References

[1] N. Epstein, Fouling in Heat Exchangers, In: Proc. of the 6th Int. heat transfer conference, 1978, pp. 235–253.
[2] E. Dalas, P.G. Koutsoukos, The effect of magnetic fields on calcium carbonate scale formation, J. Cryst. Growth, 96 (1989) 802–806.
[3] S. Kobe, G. Dražić, A.C. Cefalas, E. Sarantopoulou, J. Stražišar, Nucleation and crystallization of $CaCO_3$ in applied magnetic fields, Cryst. Eng., 5 (2002) 243–253.
[4] F. Alimi, M. Tlili, M. Ben Amor, C. Gabrielli, G. Maurin, Influence of magnetic field on calcium carbonate precipitation, Desalination, 206 (2007) 163–168.
[5] X. Miao, L. Xiong, J. Chen, Z. Yang, W. He, Experimental study on calcium carbonate precipitation using electromagnetic field treatment, Water Sci. Technol., 67 (2013) 2784–2790.
[6] H.F. An, Z.A. Liu, J.D. Zhao, X. Zhang, S. Long, J. Zhao, T. Xia, X. Zhang, Scale inhibition effects and mechanism of high voltage electrostatic fields in thermal power plant circulating cooling water system, Chin. J. Environ. Eng., 7 (2013) 4295–4299 (in Chinese).
[7] J.D. Zhao, Z.A. Liu, E.J. Zhao, Combined effect of constant high voltage electrostatic field and variable frequency pulsed electromagnetic field on the morphology of calcium carbonate scale in circulating cooling water systems, Water Sci. Technol., 70 (2014) 1074–1082.
[8] S.H. Lee, A Study of Physical Water Treatment Technology to Mitigate the Mineral Fouling in a Heat Exchanger, PhD Thesis, Drexel University, Michigan, USA, 2002.
[9] L. Jiang, J. Zhang, D. Li, Effects of permanent magnetic field on calcium carbonate scaling of circulating water, Desal. Wat. Treat., 53 (2013) 1275–1285.
[10] F. Alimi, M.M. Tlili, M. Ben Amor, G. Maurin, C. Gabrielli, Effect of magnetic water treatment on calcium carbonate precipitation: influence of the pipe material, Chem. Eng. Process., 48 (2009) 1327–1332.
[11] Y.M. Al-Roomi, K.F. Hussain, M. Al-Rifaie, Performance of inhibitors on $CaCO_3$ scale deposition in stainless steel & copper pipe surface, Desalination, 375 (2015) 138–148.
[12] T.M. Pääkkönen, M. Riihimäki, C.J. Simonson, E. Muurinen, R.L. Keiski, Crystallization fouling of $CaCO_3$ – analysis of experimental thermal resistance and its uncertainty, Int. J. Heat Mass Transfer, 55 (2012) 6927–6937.
[13] T.M. Pääkkönen, M. Riihimäki, C.J. Simonson, E. Muurinen, R.L. Keiski, C Modeling $CaCO_3$ crystallization fouling on a heat exchanger surface – definition of fouling layer properties and model parameters, Int. J. Heat Mass Transfer, 83 (2015) 84–98.
[14] N. Andritsos, A.J. Karabelas, Calcium carbonate scaling in a plate heat exchanger in the presence of particles, Int. J. Heat Mass Transfer, 46 (2003) 4613–4627.
[15] R. Liu, A Study of Fouling in a Heat Exchanger with an Application of an Electronic Anti-fouling Technology, Ph.D. Thesis, Drexel University, USA, 1999.
[16] M. Ferreux, Role d'un traitement magnétique sur la cristallogénèse du carbonate de calcium dans les eaus entartrantes, Ph.D. Thesis, Besancon, France, 1992.
[17] J.W. Mullin, Crystallization, Beijing: World Publishing Corporation, 2000, pp. 123–129.
[18] O. Lopez, P. Zuddas, D. Faivre, The influence of temperature and seawater composition on calcite crystal growth mechanisms and kinetics: implications for Mg incorporation in calcite lattice, Geochim. Cosmochim. Acta, 73 (2009) 337–347.
[19] S. Zhong, A. Mucci, Calcite precipitation in seawater using a constant addition technique: a new overall reaction kinetic expression. Geochim. Cosmochim. Acta, 57 (1993) 1409–1417.
[20] A. Mucci, Growth kinetics and composition of magnesian calcite overgrowths precipitated from seawater: quantitative influence of orthophosphate ions, Geochim. Cosmochim. Acta, 50 (1986) 2255–2265.
[21] A. Mucci, R. Canuel, S. Zhong, The solubility of calcite and aragonite in sulfate-free seawater and the seeded growth kinetics and composition of the precipitates at 250°C, Chem. Geol., 74 (1989) 309–320.
[22] A.E. Nielsen, Kinetics of Precipitation, Pergamon Press, New York, 1964, pp. 11–19.